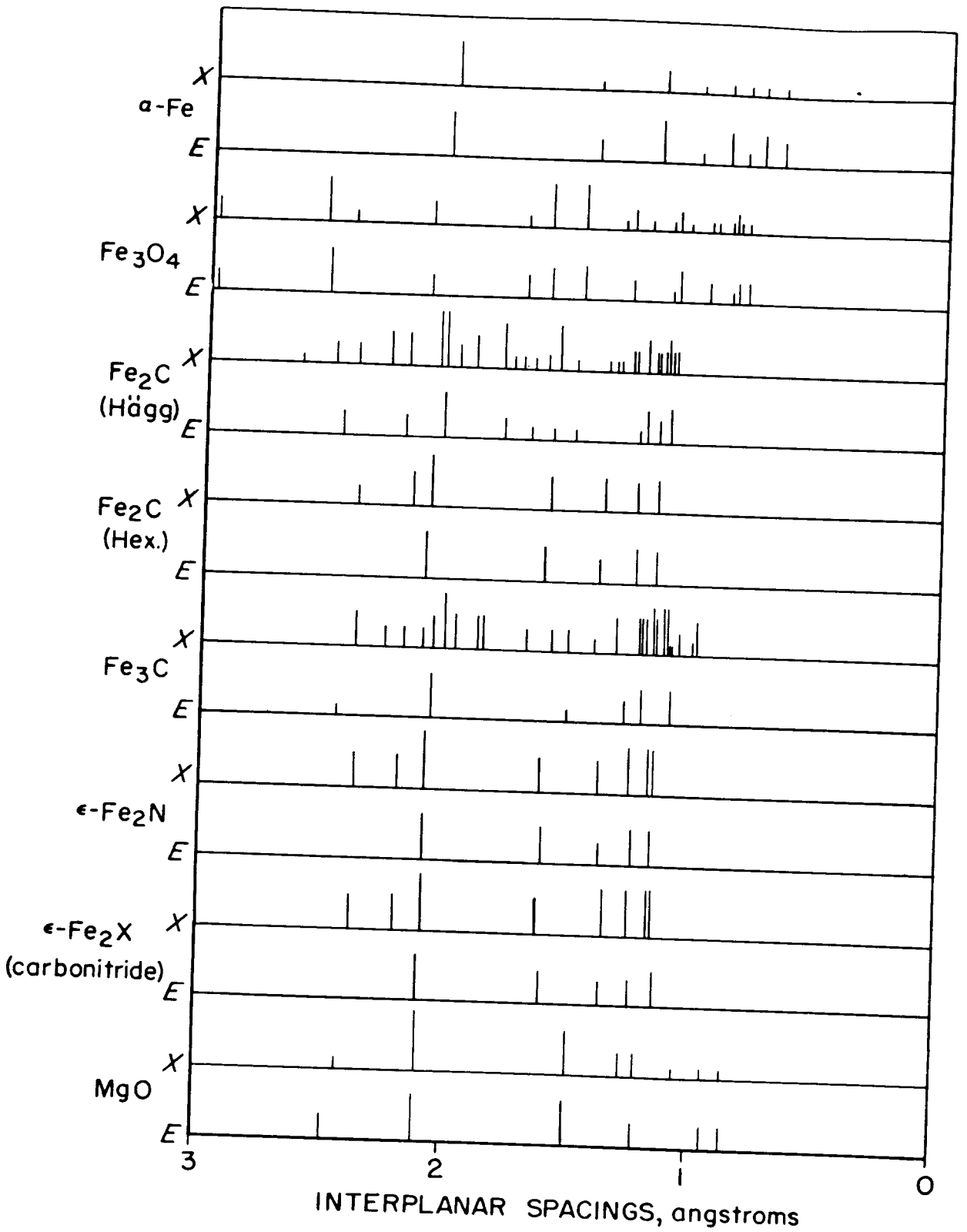

FIGURE 34.—Comparison of X-ray (*X*)- and Electron (*E*)-Diffraction Patterns of Phases in Iron Fischer-Tropsch Catalysts.

TABLE 25.—*Comparison of X-ray- and electron-diffraction patterns of phases in iron Fischer-Tropsch Catalysts* [1]

Diffraction			
Electron		X-ray	
d/n	I/I₁	d/n	I/I₁
α-Fe [2]			
2. 03	s	2. 01	1. 00
1. 43	w	1. 428	. 15
1. 17	s	1. 166	. 38
1. 02	vw	1. 010	. 10
. 903	m	. 904	. 08
. 829	vw	. 825	. 03
. 767	m	. 764	. 10
. 674	w	. 676	. 03
Fe_3O_4 [2]			
2. 97	w	2. 97	0. 28
2. 52	s	2. 53	1. 00
		2. 42	. 11
2. 10	w	2. 10	. 32
1. 71	w	1. 71	. 16
1. 61	m	1. 61	. 64
1. 48	m	1. 483	. 80
		1. 326	. 06
1. 28	w	1. 279	. 20
		1. 210	. 05
1. 12	vw	1. 121	. 10
1. 09	m	1. 092	. 32
		1. 049	. 10
. 971	w	. 970	. 16
		. 940	. 06
. 877	vw	. 880	. 10
. 857	w	. 859	. 20
		. 853	. 08
. 809	w	. 814	. 10
Fe_2C (HÄGG) [3]			
		2. 62	vw
2. 45	w	2. 48	w
		2. 39	w
		2. 26	m
2. 19	w	2. 18	m
		2. 06	vs
2. 04	s	2. 03	vs
		1. 98	w br
		1. 91	m
1. 79	w	1. 80	s
		1. 76	vw
		1. 72	vw
1. 68	vw	1. 67	vw
		1. 62	vw
1. 59	vw	1. 57	s
1. 50	vw	1. 50	vw
		1. 37	vw
		1. 34	vw
		1. 32	vw
		1. 27	w
1. 24	vw	1. 25	w
1. 21	m	1. 21	m
		1. 17	w
1. 16	w	1. 16	w
		1. 14	w
1. 11	m	1. 13	m
		1. 11	w br
		1. 09	w br
Fe_2C (hex.) [3]			
		2. 38	w
		2. 16	m
2. 10	s	2. 08	vs
1. 61	m	1. 60	m
1. 39	w	1. 37	m
1. 24	m	1. 24	m
1. 16	m	1. 16	m

Diffraction			
Electron		X-ray	
d/n	I/I₁	d/n	I/I₁
Fe_3C [3]			
2. 45	vw	2. 37	m
		2. 25	w
		2. 18	w
		2. 10	w
2. 06	s	2. 06	m
		2. 01	vs
		1. 97	m
		1. 87	m
		1. 85	m
		1. 68	w
		1. 58	w
1. 51	vw	1. 51	w
		1. 403	vw
1. 28	w	1. 322	m
		1. 222	m
1. 21	m	1. 214	m
		1. 189	m
		1. 159	s
		1. 149	m
		1. 124	s
1. 09	m	1. 104	s
		1. 096	vw
		1. 087	vw
		1. 052	w
		1. 002	vw
		. 986	m br
ε-Fe_2N [4]			
		2. 37	m
		2. 19	m
2. 08	s	2. 08	vs
1. 60	m	1. 61	m
1. 37	w	1. 375	m
1. 24	m	1. 25	s
		1. 17	s
1. 16	m	1. 15	s
		1. 10	vw
		1. 05	w
		1. 00	w
ε-Fe_2X [4, 5] **(CARBONITRIDE)**			
		2. 37	m
		2. 19	m
2. 09	s	2. 08	vs
1. 60	m	1. 615	m
1. 36	w	1. 37	s
1. 24	w	1. 25	s
		1. 17	s
1. 14		1. 15	s
		1. 10	vw
		1. 05	w
		1. 00	w
MgO [2]			
2. 45	w	2. 42	0. 06
2. 10	s	2. 10	1. 00
1. 49	s	1. 485	. 75
		1. 266	. 06
1. 21	w	1. 213	. 15
		1. 050	. 04
. 936	w	. 94	. 10
. 857	w	. 86	. 04

[1] *d/n*=interplanar spacing in Angstroms; *I/I₁*=estimated relative intensity; s=strong; m=medium; w=weak; v=very; br=broad.
[2] X-ray data from Hanawalt, Rinn and Frevel, reference (*45*).
[3] X-ray data from Hofer, Cohn and Peebles, reference (*50*).
[4] Contains a trace of magnetite.
[5] C:Fe atom ratio=0.16; N:Fe atom ratio=0.37.

be made from it (*18*). Metals prepared by reducing catalysts at temperatures so far below the melting point and in the presence of promoters are probably highly disordered and stressed. The interstitial phases derived from such metals will also be highly stressed. Furthermore the structures of the interstitial compounds of iron are much more susceptible to stress, and the results of stress will be much more dramatic than in the case of the original metal. This conclusion derives from the Hägg classification (*41*) of interstitial compounds into the stable and unstable forms, depending on whether the ratio of the carbon atom radius to the metal atom radius is less than or greater than about 0.58. The interstitial iron compounds belong to the unstable group and reflect this instability by the relatively low temperatures at which they either decompose or rearrange to form new phases, the large number of structures which they can assume, and the relative complexity of some of these structures. Apparently surface disorder can be observed only by electron diffraction.

TABLE 26.—*X-ray- and electron-diffraction data of pretreated iron catalysts*

Experiment	Catalyst		Pretreatment [2]	Phases indicated by [3]	
	Number	Type [1]		X-ray diffraction	Electron diffraction
29–1	D3001	*F*	*R, C*	χ	MgO.
30–1	D3001	*F*	*R*	α	MgO.
2			*R, C*	χ	MgO.
3			*R, C, R*	α	MgO.
4			*R, C*	α, χ	MgO.
32–1	P3003.1	*P*	*R, C, R*	α, Cu	α, *M*.
2			*R, C*	ϵ-*C*	ϵ-*C*, *M*.
3			*R*	α, Cu	α, (?).
4			*R, C*	ϵ-*C*, α	ϵ-*C*.
36–1	P3003.1	*P*	*R*	α, Cu	α, *M*.
2			*R, C*		ϵ-*C*.
3			*R, C*	α, ϵ-*C*	ϵ-*C*.
4			*R, C*	ϵ-*C*, Cu	ϵ-*C*.
4II			*R, C, T*	*C*	*C*.
43–3	P3002	*P*	*R, C*	ϵ-*C*, α	*M*, ϵ-*C*.
4			*R, C*	ϵ-*C*, α	ϵ-*C*.
45–1	P3002.1	*P*	*C*	*M*, χ	*M*.
4			*C*	*M*, χ	*M*.
46–1	P3002.1	*P*	*C*	χ, *M*	χ.
4			*C*	*M*, ϵ-*C*	*M*.
47–1	P3002.1	*P*	*R, C*	χ, (*M*?)	χ.
2			*R, C*	χ, *M*	χ.
3			*R, C*	χ, *M*	χ.
4			*R, C*	*M*, χ	*M*.
48–1	P3002.1	*P*	*R, C, R*	α, χ	α.
2			*R, C, R, C, R*	α, χ	α.
3			*R, C, R*	α, χ	α.
	A–2106.052	*S*	*R, C*	χ	*M*.
N–32	A–2106.05	*S*	*R, N*	ϵ-*N*	ϵ-*N*.
N–40	D–3001	*F*	*R, N*	ϵ-*N*	ϵ-*N*, MgO.

[1] *F*=fused; *P*=precipitated; *S*=sintered.
[2] *R*=reduced in H_2; *C*=carburized in CO; *T*=heat treatment in helium or vacuum at 450° C. *N*=nitrided in NH_3.
[3] α=metallic iron; *M*=magnetite; χ=Hägg carbide; *C*=cementite; ϵ-*C*=hexagonal iron carbide; ϵ-*N*=hexagonal iron nitride; MgO=magnesia and Cu=copper. Phases are listed in order of decreasing intensities of diffraction patterns; questionable patterns are marked (?).

In tables 26 to 28 the phases are reported in order of decreasing intensity of diffraction patterns. When the diffraction pattern was very weak or when many lines were missing, the reported phases were indicated in the tables as questionable.

TABLE 27.—*X-ray- and electron-diffraction data of fused catalyst, D3001, taken during the synthesis*

($1H_2$+1CO gas at 7.8 atmospheres.)

Testing, days	Average temperature °C.	Phases identified by [1]	
		X-ray diffraction	Electron diffraction
TEST X194, CATALYST REDUCED			
0		α	MgO, α
2	234	α, *M*	MgO, *M*.
8	258	α, *M*, χ	MgO, *M*.
22	258		MgO, *M*.
50	257	α, *M*, χ	MgO, *M*.
64	257	*M*, χ, α	*M*, MgO.
79	256	*M*, χ, α	*M*, MgO.
90	272	*M*, χ, α	*M*, MgO.
97	300	*M*, χ, α	*M*, MgO.
TEST X294, CATALYST REDUCED AND CARBURIZED TO HÄGG CARBIDE			
0		χ, α	MgO.
2	210	χ, α	MgO.
12	230	χ, α, *M*?	MgO.
54	228	χ, *M*	MgO, (?).
61	229	χ, *M*	MgO, (?).
68	228	χ, *M*	MgO, (?).
89	229	χ, *M*	MgO.
TEST X317, CATALYST REDUCED, PARTIALLY CARBURIZED TO HÄGG CARBIDE, THEN HEATED TO PRODUCE CEMENTITE			
0		C	MgO.
4	220	C	MgO.
10	230	C	MgO.
24	231	C	MgO.
42	234	C, *M*	MgO.
56	236	C, *M*	MgO, (M?).
70	237	C, *M*	MgO, (M).
84	237	C, *M*	MgO, (M?).

[1] α=metallic iron; *M*=magnetite; χ=Hägg carbide; *C*=cementite; MgO=magnesia. Phases listed in order of decreasing intensities of diffraction patterns; questionable patterns are marked (?).

The data of table 26 (obtained with specimens that were not used for synthesis) indicate that iron and iron carbides in precipitated catalysts were usually identified by both electron and X-ray diffraction. Hägg carbide in these catalysts was obtained by both methods, regardless of whether the oxides were first reduced and then carburized or whether they were carburized directly. In a few cases the less intense pattern was not found by one or the other method. However, the electron-diffraction pat-

TABLE 28.—*Phases indicated by X-ray and electron diffraction of used Fischer-Tropsch catalysts*

(All tests with $1H_2+1CO$ gas unless otherwise noted)

Catalyst type and No.	Test No. X—	Pretreatment [1]	Synthesis conditions: Pressure, atmospheres	Synthesis conditions: Average temperature, ° C.	Synthesis conditions: Testing, weeks	Phases indicated by [2]—: X-ray diffraction	Phases indicated by [2]—: Electron diffraction
Fused:							
D3001	100	*R*	7.8	267	6	*M*, α	*M*, (MgO?).
	152	*R*	7.8	270	7	*M*, α, χ	*M*, (MgO?).
	162	*R*	7.8	250	5	*M*, χ, α	*M*, (MgO?).
	225	*R*, *N*	21.4	236	15	ϵ-*CN* [4]	ϵ-*CN* (?[4]), (?), *M*(?).
	236	*R*, *N*	[3] 7.8	230	7	ϵ-*CN* [4]	MgO, *M*.
	275	*R*, *N*	1.0	265	3		
			7.8	228	6	ϵ-*CN* [4]	MgO, *M*.
	286	*R*, *N*, *C*	7.8	219	6	ϵ-CN [4]	MgO, *M*.
	289	*R*, *C*	7.8	229	28	χ, (*M*?)	MgO, (?).
	327	*R*, *N*	[3] 21.4	212	9	ϵ-*CN*, [4] (*M*?)	(?).
D3008	253	*R*, *N*	7.8	230	7	ϵ-*CN* [4]	*M*?, (ϵ-*CN*?[4]).
A2102	164	*R*	7.8	286	4	*M*, α, χ	*M*.
Sintered:							
A2101	166	*R*	7.8	234	7	χ, *M*	*M*.
A2106.11	266	*R*, *N*	7.8	216	6	ϵ-*CN* [4]	ϵ-*CN*, [4] *M*.
A2106.052	389	*R*, *C*	7.8	210	5	χ, *M*, *S*	(?).
Cemented:							
A3213.24	131	*R*	7.8	232	4	α, χ, *M*	(?[5]).
A3215	138	*R*	7.8	242	6	α, *M*, χ	(?[5]).
A3218.20	186	*R*	7.8	264	1	χ	(?[5]).
Precipitated:							
L2002	119	*I*	7.8	244	5	*M*, χ	*M*.
LH3001	81	*I*	7.8	233	9		*M*.
P3003.05	86	*I*	7.8	236	10		*M*.
P3003	87	*I*	7.8	250	11		*M*.
P3003.24	143	None	7.8	236	5	*M*, ϵ-*C*, [4] Cu	*M*.
	245	*R*	7.8	229	7	ϵ-*C*, [4] *M*, Cu, χ	(?).
	273	*R*, *N*	7.8	229	6	ϵ-*CN*, [4] Cu	ϵ-*CN*. [4]
	324	*R*, *C*	7.8	229	8	χ, *S*	*M*, (?).

[1] *R*=reduced in H_2; *N*=nitrided in NH_3; *C*=carburized in CO; *I*=inducted in synthesis gas.

[2] α=metallic iron; *M*=magnetite; χ=Hägg carbide; ϵ-*C*=hexagonal carbide; ϵ-*CN*=ϵ-carbonitride, *S*=siderite, MgO=magnesia. Phases listed in order of decreasing intensities of diffraction patterns; questionable patterns are marked (?).

[3] $1H_2+1.5CO$ gas used.

[4] Diffraction patterns of hexagonal carbide and ϵ-carbonitride are essentially indistinguishable. One or the other phase is indicated depending on which phase is the more probable in the light of its previous history.

[5] Possibly an alumina phase or phases.

terns of iron carbides were not obtained with reduced and carburized catalysts that originally contained massive, nonporous magnetite. Thus, a carburized sintered catalyst (A2106.052) produced the electron-diffraction pattern of magnetite, whereas X-ray diffraction indicated the presence of Hägg carbide only. Although X-ray diffraction patterns of many samples of a reduced and carburized fused catalyst (D3001) indicated the presence of iron and Hägg carbide, electron-diffraction patterns usually contained only the lines of the structural promoter, magnesium oxide. Only in the first sample of test X194 with a fused catalyst (table 27) were electron-diffraction lines of iron observed in addition to those of magnesium oxide. However, lines of ϵ-nitride were found in the electron-diffraction patterns of sintered and fused catalysts that had been nitrided.

Similarly, the examination by electron diffraction of samples of a fused catalyst (D3001), removed from the reactor at various intervals during the synthesis, showed the pattern of magnesia most prominently; however, the magnetite pattern was also observed (table 27). In test X194, X-ray and magnetic analyses (*10*) indicated the relatively rapid formation of at least 20 percent of Hägg carbide and a slower rate of formation of magnetite. However, the Hägg carbide content reached its maximum and decreased slowly after about 8 days, whereas the magnetite content increased throughout the testing. The electron-diffraction data indicated the presence of magnetite even in the reduced catalyst. The magnetite pattern increased in intensity and became more intense than that of magnesia after 9 weeks of synthesis.

In test X294 (table 27) the same catalyst (D3001) was converted to Hägg carbide before use in the synthesis. (See table 8 for magnetic analysis.) Magnetite lines were ob-

served by X-rays after 12 days of testing, but these remained secondary to the Hägg carbide lines throughout the test. With the exception of several unidentified lines found in three of the samples, only magnesia lines were found by electron diffraction. Thus, both X-ray and electron diffraction indicated that this carbided catalyst was oxidized at a slower rate than the reduced catalyst.

Similar results were obtained in test X317, in which this catalyst was converted to cementite before the synthesis. (See table 9 for magnetic analysis.) Here again, both X-ray and electron diffraction indicated a slower rate of oxidation than for the reduced catalyst. The electron-diffraction pattern contained only lines of magnesia for the first 42 days of the test; after this period, weak lines of magnetite appeared in addition. The precarbided samples of this fused catalyst were considerably more active than the reduced one.

Data from other tests of catalyst D3001 (table 28) are similar to those in table 27. After several weeks of use in synthesis, samples that were reduced initially (tests X100, X152, and X162) produced the electron patterns of magnetite and possibly magnesia, while X-ray analysis indicated the presence of Hägg carbide and iron in addition to magnetite. A sample that was initially converted to Hägg carbide (X289) produced the electron-diffraction pattern of magnesia plus some unidentified lines. Fused catalysts D3001 and D3008 were reduced and nitrided before use in tests X225 and X253. In the synthesis the ϵ-iron nitride was converted to ϵ-iron carbonitride, and no magnetite was found by X-ray diffraction. The electron-diffraction lines were difficult to interpret but appeared to be those of ϵ-iron carbonitride and magnetite. In tests X236, X275, and X327, catalyst D3001 was reduced and nitrided. However, after synthesis, lines corresponding to the ϵ-iron nitride or carbonitride phases were not found in the electron-diffraction pattern. In test X286 this catalyst was reduced, partially nitrided, and carburized to form an ϵ-carbonitride, but the electron-diffraction pattern of the ϵ-phase was not obtained from the used catalyst.

The results with sintered catalysts were similar to those obtained with fused catalysts. After synthesis a sample that had been reduced initially (X166) produced the electron-diffraction pattern of magnetite only, whereas X-ray analysis indicated Hägg carbide as the major phase. A used, initially carburized, sintered catalyst produced an electron-diffraction pattern that could not be identified (X389). A used, sintered catalyst that had been nitrided (X266) produced patterns of ϵ-carbonitride and magnetite by both electron and X-ray diffraction.

A used, cemented catalyst (X186) showed an exceptionally sharp and well defined X-ray pattern of Hägg carbide. Its electron-diffraction pattern contained only unidentified lines. Catalysts of this type were made by cementing a magnetite powder into coherent granules with alumina from aluminum nitrate. Hence, each particle of iron oxide was surrounded by a coating of alumina, and thus it is not unreasonable to attribute the observed lines to an alumina phase.

Precipitated catalysts that were inducted in synthesis gas produced the electron-diffraction pattern of magnetite only, although in test X143 the X-ray-diffraction patterns of hexagonal iron carbide and copper were also observed. The electron-diffraction pattern of a reduced, precipitated catalyst (X245) could not be identified, and the pattern of the reduced and carbided, precipitated catalyst (X324) was also difficult to identify but appeared to contain the lines of magnetite. The reduced and nitrided catalyst used in test X273 produced electron and X-ray-diffraction patterns of ϵ-carbonitride.

The experimental results may be summarized as follows:

1. For reduced, carbided, or nitrided catalysts of precipitated iron, electron and X-ray diffraction indicated the presence of the same phases. The electron- and X-ray-diffraction patterns of interstitial compounds are similar, but have some characteristic differences.
2. After use in the synthesis and extraction, precipitated-iron catalysts usually produced electron-diffraction patterns of magnetite only, even though the X-ray-diffraction patterns contained lines of Hägg carbide and/or hexagonal iron carbide. Only a used, precipitated catalyst that was reduced and nitrided showed an interstitial phase, ϵ-carbonitride, by both electron and X-ray diffraction.
3. After suitable pretreatment or use in the synthesis, fused catalysts containing magnesia usually produced electron-diffraction patterns of magnesia or magnetite, although X-ray diffraction indicated the presence of metallic iron, Hägg carbide, and/or cementite. The only interstitial phases identified by electron diffraction were nitrides and carbonitrides.
4. Nitrides and carbonitrides were the only phases detectable by electron diffraction of sintered and cemented catalysts.

An interesting result of these studies is the apparent absence of iron carbides in the surface layers of used Fischer-Tropsch catalysts. However, interpretation of the data is complicated by the following factors:

1. If the carbide consists of small and/or highly disordered crystallites, it may produce either indistinct electron-diffraction patterns or patterns that are considerably different from those of the bulk phases.
2. Unidentified lines found in some of the electron-diffraction patterns may correspond to an unknown iron carbide or a related phase. However, no lines corresponding to the carbide reported by Eckstrom and Adcock (*30*) were found by either electron or X-ray diffraction.

3. With sintered or fused catalysts, electron-diffraction patterns of carbides were not obtained, although X-ray and magnetic analyses indicated that Hägg carbide or cementite was the principal phase in a given sample. However, since the electron pattern due to magnetite either appeared or became more intense during synthesis, it must be inferred that iron or some of its compounds in some amorphous form is present in the surface. In some cases, catalysts converted to ϵ-iron nitride produced the electron-diffraction pattern of the ϵ phase after both pretreatment and use in the synthesis. Hence the ϵ-phase must be present near the surface as moderately large and ordered crystallites.

Considerable attention has been given to the role of carbide in the synthesis (*28, 59, 80, 86*). Although this section presents no direct evidence concerning surface carbide, the presence of magnetite and apparent absence of carbides near the surface of active used iron catalysts does not add support to the already questionable carbide theory. In most tests, catalytic activity and selectivity remained essentially constant over periods in which the surface layers as well as the bulk of the catalyst were converted to magnetite, so that magnetite may be a principal surface phase in the synthesis. This is not so with nitrided catalysts, and the activity and selectivity of such catalysts show marked differences from those of inducted, reduced, or carbided catalysts.

The prominence of the electron-diffraction pattern of magnesia in fused catalysts containing magnesia indicates the presence of the structural promoter at the surface of the catalysts. Since the diameters of crystallites required to produce a satisfactory electron-diffraction pattern must exceed 30 Å., magnesia does not appear to be dispersed molecularly in reduced catalysts, but must be present in moderately large crystallites. Although the crystallites of magnesia are larger than expected, these results are not necessarily contradictory to the present concepts of the role of structural promoters in fused-magnetite catalysts (*43*).

Chemical analyses of used catalysts described in a previous section indicate that part of the magnesia promoter in catalyst D3001 was converted to magnesium carbonate during synthesis. This reaction proceeds more rapidly at higher synthesis pressures, the conversion to magnesium carbonate being small at 7.8 atmospheres and large at 21.4 atmospheres. Table 28 shows that electron-diffraction patterns of MgO were found in all samples of catalyst D3001 used in synthesis at 7.8 atmospheres, but not in the two samples used at 21.4 atmospheres.

BIBLIOGRAPHY [17]

1. ACKERMANN, P. [Latest German Developments on the Gas Phase. Gasoline Synthesis at Middle Pressures, 1942–1945.] FIAT Reel X–116, Frames 1717–1787.
2. ALMQUIST, J. A., and BLACK, C. A. The Poisoning Action of Oxygen on Iron Catalysts for Ammonia Synthesis. Jour. Am. Chem. Soc., vol. 48, 1926, pp. 2814–2820.
3. ANDERSON, J. A., and SEYFRIED, W. D. Determination of Oxygenated and Olefin Compound Types by Infrared Spectroscopy. Anal. Chem., vol. 20, 1948, pp. 998–1006.
4. ANDERSON, R. B. Improved Adsorption Vessel. Ind. Eng. Chem., Anal. Ed., vol. 18, 1946, p. 156.
5. ———. Iron Nitrides as Fischer-Tropsch Catalysts. Advances in Catalysis, Academic Press, Inc., New York, N.Y., vol. 5, 1953, pp. 355–384.
6. ———. Kinetics and Reaction Mechanism of the Fischer-Tropsch Synthesis. Chap. 3 in Catalysis, ed. by P. H. Emmett, Reinhold Pub. Corp., New York, N.Y., vol. 4, 1956, pp. 257–372.
7. ANDERSON, R. B., HALL, W. K., HEWLETT, H. D., and SELIGMAN, B. Studies of the Fischer-Tropsch Synthesis. II. Properties of Unreduced Cobalt Catalysts. Jour. Am. Chem. Soc., vol. 69, 1947, pp. 3114–3119.
8. ANDERSON, R. B., HALL, W. K., and HOFER, L. J. E. Studies of the Fischer-Tropsch Synthesis. IV. Properties of Reduced Cobalt Catalysts. Jour. Am. Chem. Soc., vol. 70, 1948, pp. 2465–2472.
9. ANDERSON, R. B., HALL, W. K., KRIEG, A., and SELIGMAN, B. Studies of the Fischer-Tropsch Synthesis. V. Activities and Surface Areas of Reduced and Carburized Cobalt Catalysts. Jour. Am. Chem. Soc., vol. 71, 1949, pp. 183–188.
10. ANDERSON, R. B., HOFER, L. J. E., COHN, E., and SELIGMAN, B. Studies of the Fischer-Tropsch Synthesis. IX. Phase Studies of Iron Catalysts in the Synthesis. Jour. Am. Chem. Soc., vol. 73, 1951, pp. 944–946.
11. ANDERSON, R. B., KRIEG, A., SELIGMAN, B., and O'NEILL, W. E. Fischer-Tropsch Synthesis. I. Tests of Cobalt Catalysts at Atmospheric Pressure. Ind. Eng. Chem., vol. 39, 1947, pp. 1548–1554.
12. ANDERSON, R. B., McCARTNEY, J. T., HALL, W. K., and HOFER, L. J. E. Kieselguhrs—Suitability as Carriers in Catalysts. Ind. Eng. Chem., vol. 39, 1947, pp. 1618–1628.
13. ANDERSON, R. B., SELIGMAN, B., SHULTZ, J. F., KELLY, R., and ELLIOTT, M. A. The Fischer-Tropsch Synthesis. Some Important Variables of the Synthesis Over Iron Catalysts. Ind. Eng. Chem., vol. 44, 1952, pp. 391–397.
14. ANDERSON, R. B., and SHULTZ, J. F. Iron Nitride Catalyst in Carbon Oxide Hydrogenation. U.S. Patent 2,629,728, Feb. 24, 1953.
15. ANDERSON, R. B., SHULTZ, J. F., HOFER, L. J. E., and STORCH, H. H. Physical Chemistry of the Fischer-Tropsch Synthesis. Bureau of Mines Bull. 580, 1959, 25 pp.
16. ANDERSON, R. B., SHULTZ, J. F., SELIGMAN, B., HALL, W. K., and STORCH, H. H. Studies of the Fischer-Tropsch Synthesis. VII. Nitrides of Iron as Catalysts. Jour. Am. Chem. Soc., vol. 72, 1950, pp. 3502–3508.
17. BEECK, O. Catalysis—A Challenge to the Physicist. Rev. Modern Phys., vol. 17, 1945, pp. 61–71.
18. BRADSHAW, B. D. A Study of Metallic Electrodes Prepared by Sublimation. Jour. Chem. Phys., vol. 19, 1951, pp. 1026–1027.
19. BRIDGER, G. L., POLE, G. R., BEINLICH, W. A., and THOMPSON, H. L. Production and Performance of Ammonia-Synthesis Catalyst. Chem. Eng. Progress, vol. 43, 1947, pp. 291–302.
20. BROWN, H. C. Studies in Stereochemistry. V. The Effect of F-Strain on the Relative Base Strength of Ammonia and Trimethylamine. Jour. Am. Chem. Soc., vol. 67, 1945, pp. 374–378.
21. BROWNING, L. C., DEWITT, T. W., and EMMETT, P. H. Equilibria in the Systems Fe_2C-Fe-CH_4-H_2 and Fe_2C-Fe-CH_4-H_2. Jour. Am. Chem. Soc., vol. 72, 1950, pp. 4211–4217.
22. BRUNAUER, S., and EMMETT, P. H. Use of Low-Temperature van der Waal's Adsorption Isotherms in Determining the Surface Areas of Various Adsorbents. Jour. Am. Chem. Soc., vol. 59, 1937, pp. 2682–2689.
23. ———. Chemisorptions of Gases on Iron-Synthetic Ammonia Catalysts. Jour. Am. Chem. Soc., vol. 62, 1940, pp. 1732–1746.
24. BRUNAUER, S., EMMETT, P. H., and TELLER, E. Adsorption of Gases in Multimolecular Layers. Jour. Am. Chem. Soc., vol. 60, 1938, pp. 309–319.
25. BRUNAUER, S., JEFFERSON, M. E., EMMETT, P. H., and HENDRICKS, S. B. Equilibria in the Iron-Nitrogen System. Jour. Am. Chem. Soc., vol. 53, 1931, pp. 1778–1786.
26. CLARK, E. L., KALLENBERGER, R. H., BROWN, R., and PHILLIPS, J. R. Synthesis-Gas Production; Reaction of Light Hydrocarbons, Steam, and Carbon Dioxide in Commercial Equipment. Chem. Eng. Prog., vol. 45, 1949, pp. 651–654.
27. COHN, E. M., and HOFER, L. J. E. Mode of Transition from Hägg Iron Carbide to Cementite. Jour. Am. Chem. Soc., vol. 72, 1950, pp. 4662–4664.
28. CRAXFORD, S. R., and RIDEAL, E. K. Mechanism of the Synthesis of Hydrocarbons from Water Gas. Jour. Chem. Soc., 1939, pp. 1604–1614.
29. CROWELL, J. H., BENSON, H. E., FIELD, J. H., and STORCH, H. H. Fischer-Tropsch Oil-Circulation Processes. Ind. Eng. Chem., vol. 42, 1950, pp. 2376–2384.
30. ECKSTROM, H. C., and ADCOCK, W. A. New Iron Carbide in Hydrocarbon-Synthesis Catalysts. Jour. Am. Chem. Soc., vol. 72, 1950, pp. 1042–1043.
31. EISENHUT, O., and KAUPP, E. [Radiographic Investigation of the System, Iron-Nitrogen.] Ztschr. Elektrochem., vol. 36, 1930, pp. 392–404.
32. EMMETT, P. H., and BRUNAUER, S. Adsorption of Nitrogen by Iron-Synthetic-Ammonia Catalysts. Jour. Am. Chem. Soc., vol. 56, 1934, pp. 35–41.
33. ———. Accumulation of Alkali Promoters on Surfaces of Iron Synthetic Ammonia Catalysts. Jour. Am. Chem. Soc., vol. 59, 1937, pp. 310–315.
34. ———. The Use of Low Temperature van der Waal's Adsorption Isotherms in Determining the Surface Area of Iron Synthetic Ammonia Catalysts. Jour. Am. Chem. Soc., vol. 59, 1937, pp. 1553–1564.

[17] Titles enclosed in brackets are translations from the language in which the item was published.

35. EMMETT, P. H., and DEWITT, T. W. The Low Temperature Adsorption of Nitrogen, Oxygen, Argon, Hydrogen, *n*-Butane and Carbon Dioxide on Porous Glass and on Partially Dehydrated Chabazite. Jour. Am. Chem. Soc., vol. 65, 1943, pp. 1253–1262.
36. EMMETT, P. H., and SHULTZ, J. F. Equilibria in the Iron-Hydrogen-Oxygen System. Indirect Calculation of the Water-Gas Equilibrium Constant. Jour. Am. Chem. Soc., vol. 52, 1930, pp. 4268–4285.
37. ———. Gaseous Thermal Diffusion—The Principal Cause of Discrepancies Among Equilibrium Measurements on the Systems Fe_3O_4-H_2-Fe-H_2O, Fe_3O_4-H_2-FeO-H_2O, and FeO-H_2-Fe-H_2O. Jour. Am. Chem. Soc., vol. 55, 1933, pp. 1376–1389.
38. EVANS, U.R. Oxidation of Iron in the Range 100°–400° C. Nature, vol. 164, 1949, pp. 909–910.
39. FISCHER, F., and TROPSCH, H. [Synthesis of Petroleum at Atmospheric Pressures from Gasification Products of Coal.] Brennstoff-Chem., vol. 7, 1926, pp. 97–104.
40. HÄGG G. X-Ray Studies on the Binary Systems of Iron with Nitrogen, Phosphorous, Arsenic, Antimony and Bismuth. Nova Acta Regiae Soc. Sci. Upsaliensis, vol. 7, 1929, pp. 1–95.
41. ——— [Regularity in Crystal Structure in Hydrides, Borides, Carbides and Nitrides of Transition Elements.] Ztschr. physik. Chem., vol. 12B, 1931, pp. 33–56.
42. HALL, W. K., DIETER, W. E., HOFER, L. J. E., and ANDERSON, R. B. Preparation and Reactions of Carbonitrides on Iron. Jour. Am. Chem. Soc., vol. 75, 1953, pp. 1442–1447.
43. HALL, W. K., TARN, W. H., and ANDERSON, R. B. Studies of the Fischer-Tropsch Synthesis. VIII. Surface Area and Pore Volume Studies of Iron Catalysts. Jour. Am. Chem. Soc., vol. 72, 1950, pp. 5436–5443.
44. ———. Studies of the Fischer-Tropsch Synthesis. XIII. Structural Changes of a Reduced Iron Catalyst on Reoxidation and on Formation of Interstitial Phases. Jour. Phys. Chem., vol. 56, 1952, pp. 688–691.
45. HANAWALT, J. D., RINN, H. W., and FREVEL, L. K. Chemical Analysis by X-Ray Diffraction Classification and Use of X-Ray Diffraction Patterns. Ind. Eng. Chem., Anal. Ed., vol. 10, 1938, pp. 457–512.
46. HOFER, L. J. E. The Preparation and Properties of Metal Carbides, with Critical Comment as to their Significance in the Fischer-Tropsch Synthesis. Bureau of Mines Rept. of Investigations 3770, 1944, 39 pp.
47. ———. Crystalline Phases and Their Relation to Fischer-Tropsch Catalyst. Chap. 4 in Catalysts, ed. by P. H. Emmett, Reinhold Pub. Corp., New York, N.Y., vol. 4, 1956, pp. 373–442.
48. HOFER, L. J. E., and COHN, E. M. Synthesis of Cementite. Jour. Chem. Phys., vol. 18, 1950, pp. 766–767.
49. ———. Thermomagnetic Determination of Hägg Carbide in Used Iron Fischer-Tropsch Catalysts. Anal. Chem., vol. 22, 1950, pp. 907–910.
50. HOFER, L. J. E., COHN, E. M., and PEEBLES, W. C. Modifications of the Carbide, Fe_2C—Their Properties and Identification. Jour. Am. Chem. Soc., vol. 71, 1949, pp. 189–195.
51. ———. Isothermal Decomposition of Nickel Carbide. Jour. Phys. and Colloid Chem., vol. 54, 1950, pp. 1161–1169.
52. JACK, J. H. Binary and Ternary Interstitial Alloys. I. Iron-Nitrogen System: The Structures of Fe_4N and Fe_2N. Proc. Roy. Soc. (London), vol. A195, 1948, pp. 34–40.
53. ———. Binary and Ternary Interstitial Alloys. II. Iron-Carbon-Nitrogen System. Proc. Roy. Soc. (London), vol. A195, 1948, pp. 41–55.
54. ———. Binary and Ternary Interstitial Alloys. III. Iron-Carbon System: The Characterization of a New Iron Carbide. Proc. Roy. Soc. (London), vol. A195, 1948, pp. 56–61.
55. KÖLBEL, H. [Gasoline Synthesis with Iron Catalysts. Part I.] FIAT Reel X–115, Frames 1182–1196, Rept. No. 74, April 23, 1938.
56 KÖLBEL, H., and ENGELHARDT, F. [Reaction Mechanism of the Fischer-Tropsch Synthesis. I.] Erdöl u. Kohle, vol. 2, 1949, pp. 52–59.
57 ———. [Reaction Mechanism of the Fischer-Tropsch Synthesis. VI. Function of Water Vapor in the Hydrogenation of Carbon Monoxide.] Erdöl u. Kohle, vol. 3, 1950, pp. 529–533.
58. KRIEG, A., DUDASH, A., and ANDERSON, R. B. Improved Caustic Scrubber. Ind. Eng. Chem., vol. 41, 1949, p. 1508.
59. KUMMER, J. T., DEWITT, T. W., and EMMETT, P. H. Some Mechanism Studies on the Fischer-Tropsch Synthesis Using C^{14}. Jour. Am. Chem. Soc., vol. 70, 1948, pp. 3632–3643.
60. LEHRER, E. [Equilibrium, Iron-Hydrogen Ammonia.] Ztschr. Elektrochem., vol. 36, 1930, pp. 383–392.
61. ———. [Magnetic Investigation of the System Iron-Nitrogen.] Ztschr. Elektrochem., vol. 36, 1930, pp. 460–473.
62. McCARTNEY, J. T., and ANDERSON, R. B. Electron Microscopic Replicas Studies of Porosity in Fused Iron Catalysts. Jour. Appl. Phys., vol. 22, 1951, pp. 1441–1443.
63. McCARTNEY, J. T., HOFER, L. J. E., SELIGMAN, B., LECKY, J. A., PEEBLES, W. C., and ANDERSON, R. B. Electron and X-Ray Diffraction Studies of Iron Fischer-Tropsch Catalysts. Jour. Phys. Chem., vol. 57 1953, pp. 730–736.
64. McCARTNEY, J. T., SELIGMAN, B., HALL, W. K., and ANDERSON, R. B. An Electron Microscopic Study of Metal Oxides and Metal Oxide Catalysts. Jour. Phys. Chem., vol. 54, 1950, pp. 505–519.
65. PERRIN, M. [The Synthesis of Aliphatic Hydrocarbons]. Doctoral Diss., Univ. of Lyons, Lyons, France, 1948, 85 pp.
66. PICARD, R. B. Studies with the Electron-Microscope Diffraction Adapter. Jour. Appl. Phys., vol. 15, 1944, pp. 678–684.
67. PICHLER, H., and MERKEL, H. Chemical and Thermomagnetic Studies on Iron Catalysts for Synthesis of Hydrocarbons. Bureau of Mines Tech. Paper 718, trans. by Ruth Brinkley, 1949, 108 pp.
68. PODGURSKI, H. H., KUMMER, J. T., DEWITT, T. W., and EMMETT, P. H. Preparation, Stability and Adsorptive Properties of the Carbides of Iron. Jour. Am. Chem. Soc., vol. 82, 1950, pp. 5382–5388.
69. SCHLESINGER, H. I., BROWN, H. C., GILBREATH, J. R., and KATZ, J. J. Reaction of the Boron Halides with the Alkali Metal Hydrides and with Their Addition Compounds; A New Syntheses of Diborane. Jour. Am. Chem. Soc., vol. 75, 1953, pp. 195–199.
70. SHULTZ, J. F., ABELSON, M., SHAW, L., and ANDERSON, R. B. Fischer-Tropsch Synthesis. Nitrides and Carbonitrides of Iron as Catalysts. Ind. Eng. Chem., vol. 49, 1957, pp. 2055–2060.
71. SHULTZ, J. F., HALL, W. K., DUBS, T. A., and ANDERSON, R. B. Studies of the Fischer-Tropsch Synthesis. XV. Cementite as Catalysts. Jour. Am. Chem. Soc., vol. 78, 1956, pp. 282–285.

72. SHULTZ, J. F., HALL, W. K., SELIGMAN, B., and ANDERSON, R. B. Studies of the Fischer-Tropsch Synthesis. XIV. Hägg Carbide as a Catalyst. Jour. Am. Chem. Soc., vol. 77, 1955, pp. 213–221.
73. SHULTZ, J. F., HOFER, L. J. E., COHN, E. M., STEIN, K. C., and ANDERSON, R. B. Synthetic Liquid Fuels from Hydrogenation of Carbon Monoxide. Cobalt and Iron Catalysts for the Fischer-Tropsch Synthesis: Preparation and Characterization of Catalysts, Synthesis Tests, and Reaction Mechanism (Part 2 of Two Parts). Bureau of Mines Bull. 578, 1959, 139 pp.
74. SHULTZ, J. F., SCHOENEWEIS, F. J., and ANDERSON, R. B. Compressed Carbon Monoxide. Ind. Eng. Chem., vol. 48, 1956, p. 1365.
75. SHULTZ, J. F., SELIGMAN, B., LECKY, J. A., and ANDERSON, R. B. Studies of the Fischer-Tropsch Synthesis. XII. Composition Changes of Nitrided Iron Catalysts During Synthesis. Jour. Am. Chem. Soc., vol. 74, 1952, pp. 637–640.
76. SHULTZ, J. F., SELIGMAN, B., SHAW, L., and ANDERSON, R. B. The Fischer-Tropsch Synthesis. Effect of Nitriding on Three Types of Iron Catalyst. Ind. Eng. Chem., vol. 44, 1952, pp. 397–401.
77. STEIN, K. C., and SCHOENEWEIS, F. J. Mercury Piston Gives Close Control of Liquid Feed Rates. Chem. Eng., vol. 60, 1953, p. 200.
78. STEIN, K. C., THOMPSON, G. P., and ANDERSON, R. B. Studies of the Fischer-Tropsch Synthesis. XVII. Changes of Iron Catalysts During Pretreatment and Synthesis. Jour. Phys. Chem., vol. 61, 1957, pp. 928–932.
79. STORCH, H. H., ANDERSON, R. B., HOFER, L. J. E., HAWK, C. O., ANDERSON, H. C., and GOLUMBIC, N. Synthetic Liquid Fuels from Hydrogenation of Carbon Monoxide. Part 1—Review of Literature: Bureau of Mines Research on Effect of Catalyst Preparation, Reduction, and Induction Procedures on Activity; correlation of Physical Properties of the Catalysts With Their Activity. Bureau of Mines Tech. Paper 709, 1948, 213 pp.
80. STORCH, H. H., GOLUMBIC, N., and ANDERSON, R. B. The Fischer-Tropsch and Related Syntheses. John Wiley and Sons, New York, N.Y., 1951, 610 pp.
81. THOMPSON, J. G. Pure Carbon Monoxide for Experimental Purposes. Ind. Eng. Chem., vol. 21, 1929, pp. 389–390.
82. THOMSON, G. P., and COCHRANE, W. Theory and Practice of Electron Diffraction. The Macmillan Co., London, England, 1939.
83. TRILLAT, J. J., and OKETANI, S. [Electron-Diffraction Study of the Cementation of Iron. I. Action of Pure Carbon Monoxide.] Compt. rend., vol. 230, 1950, pp. 2203–2205.
84. ———. [Electron-Diffraction Study of the Cementation of Iron. II. Action of $CO+H_2$ Mixtures.] Compt. rend., vol. 232, 1951, pp. 1116–1118.
85. ———. [Cementation of Single Crystals of Iron.] Compt. rend., vol. 233, 1951, pp. 51–53.
86. WELLER, S., HOFER, L. J. E., and ANDERSON, R. B. The Role of Bulk Carbide in the Fischer-Tropsch Synthesis. Jour. Am. Chem. Soc., vol. 70, 1948, pp. 799–801.
87. WESTRIK, R., and ZWIETERING, P. Pseudomorphism in the Iron Synthetic Ammonia Catalyst. Proc. Koninkl. Akad. Wetenschappen Amsterdam, vol. B56, 1953, pp. 492–497.

APPENDIX A.—PREPARATION AND COMPOSITION OF CATALYSTS

Compositions of catalysts described in this bulletin are given in table A–1. Procedures for preparing these catalysts are given in the following text.

TABLE A–1.—*Catalyst composition*

(grams per 100 grams Fe)

Catalyst type and No.	K_2O	Cu	MgO	Al_2O_3	SiO_2	Cr_2O_3	ZrO_2
Fused:							
D3001	0.85	------	6.8	------	0.9	1.21	------
D3008	1.39	------	------	2.83	.28	------	------
L3028	.51	------	------	.50	.42	------	3.9
A2102	.05	------	------	------	------	------	------
Precipitated:							
L2002	.06	------	------	------	------	------	------
P3002.1	.12	0.56	------	------	------	------	------
LH3001							
P3003							
P3003.1	.5	10	------	------	------	------	------
P3003.05							
P3003.24							
Sintered:							
A2106.11	.94	.60	------	------	------	------	------
A2101	.61	------	------	------	------	------	------
Cemented:							
A3213.24	.52	------	------	5.9	------	------	------
A3215	.85	------	------	3.6	------	------	------
A3218.20	1.75	------	------	3.5	------	------	------

FUSED IRON OXIDE

Catalysts D3001, D3008, and L3028 were prepared by electrical fusion of iron oxide plus promoters. D3001 and D3008 (*19*)[1] were commercial preparations, and L3028 was prepared in our laboratory by the procedure described in an earier bulletin (*73*, p. 29). A2102 was made by reacting a heated iron powder with oxygen, and its preparation was identical to that of A2100 (*73*).

PRECIPITATED IRON OXIDE

These catalysts were precipitated from a hot aqueous solution of ferric nitrate (plus copper nitrate for catalysts promoted with copper) by adding, with stirring, a hot aqueous solution of sodium carbonate. Catalyst numbers with the prefix L were made in about 1-pound batches in laboratory-scale equipment, whereas those designated P were made in about 30-pound batches using larger equipment and a filter press. Preparation details of these catalysts have been described (*73*).

SINTERED IRON OXIDE

Agglomerates of sintered, fine particles of magnetite ore were crushed to 6- to 8-mesh impregnated with an aqueous solution of potassium nitrate (A2106.11) or potassium carbonate (A2101), and dried and heated overnight at 500° C.

CEMENTED IRON OXIDE

Fine particles of Alan Wood magnetite, super concentrate, were added to an aqueous solution of aluminum and potassium nitrates, and the mixture was evaporated to dryness (*73*). A3218.20 and A3215 were heated for 16 hours at 150° C., and A3213.24 was given the same treatment, being heated finally to 500° C. for 16 hours.

[1] Italicized numbers in parentheses refer to items in the bibliography preceding the appendixes.

APPENDIX B.—TESTING PROCEDURES

Catalyst testing apparatus and methods have been described previously (*11*, *13*, *16*, *58*, *80*). The pretreated catalysts were transferred in carbon dioxide to the synthesis reactor. Synthesis gas was passed over the catalyst, pressure was increased to the desired value, and the reactor temperature was increased rapidly to 200° C. The temperature was then increased at about 7° C. per hour until apparent contractions (CO_2-free) of about 65 percent were observed. Thereafter the temperature was varied by small increments to maintain the contraction at this value. In special experiments, the temperature was kept constant, and the contraction was held at the desired value by adjusting the flow. $1H_2+1CO$ gas was used in nearly all synthesis tests.

Catalyst tests were continuous, except for recovery of products at intervals of 1 week. Gaseous components were analyzed by a mass spectrometer. Liquid and solid hydrocarbons, including dissolved oxygenated molecules, were fractionated by a simple 1-plate distillation, and the lower boiling fractions were analyzed for functional groups by infrared spectrometry (*16*). Usually these characterizations of liquid and solid hydrocarbons were made on composite samples of products that had received from 3 to 6 weeks of testing. Average activities, A_{Fe},[1] were determined by an empirical rate equation (*13*) from weekly averages of space velocity, contraction, and temperature.

Most catalysts were analyzed after pretreatment and at the end of the synthesis test. In several experiments, the catalyst was sampled at frequent intervals by discharging the entire charge into heptane, removing 3 to 5 cc., and then returning the remaining portion to the reactor (*10*). As a precaution, the synthesis temperature was lowered about 10° C. for a brief period after sampling, because the catalyst, owing to partial extraction of high molecular weight hydrocarbons with heptane, was very active in the initial 2 or 3 hours. After a thorough extraction with boiling toluene, the catalyst samples were subjected to one or more of the following analyses: (1) Chemical analyses for iron, carbon, and nitrogen, if present, by conventional methods. From these data and the ratio of promoters to iron an estimate of oxygen content by difference was made. (2) Powder X-ray diffraction. (3) Electron diffraction on thoroughly extracted samples. (4) Thermomagnetic analyses (*49*). (5) Chemical analyses for the amount of carbon dioxide liberated upon treatment of the sample with sulfuric acid. These data are required to determine the magnitude of carbonate formation either as siderite or promoter carbonates (*75*).

The product distributions are plotted as percent of the total hydrocarbons. (The term "hydrocarbons" includes oxygenated organic molecules dissolved in the condensed hydrocarbon phases.) Total hydrocarbons are distributed into C_1, C_2, and C_3+C_4 gaseous hydrocarbons (determined by mass spectrometric analyses) and into the following distillation ranges of the condensed hydrocarbon phases: 30° to 185° C., 185° to 352° C., 352° to 464° C., and above 464° C. The percentages of olefins in the C_2 and C_3+C_4 fractions are indicated by a number following the double-bond symbol (=) in the block diagrams. Functional group analyses of the two lower distillation ranges by infrared methods (*3*) are indicated in the following manner: Br indicates the bromine number calculated from the amount of olefin; OH is the weight-percent of hydroxyl group; and CO indicates the weight-percent of carbonyl group present as aldehydes, ketones, and acids. The selectivity data are for the actual temperatures of operation given at the top of the block diagrams, whereas the activity data are corrected to 240° C.

[1] Defined as cubic centimeters of synthesis gas converted per gram of iron per hour at 240° C., when the flow is adjusted to give an apparent contraction of 65 percent.

APPENDIX C.—SEPARATION OF CARBON MONOXIDE FROM SYNTHESIS GAS

For use in pretreatment studies a relatively simple method was developed for separating carbon monoxide from compressed synthesis gas available at this laboratory (*74*). Commercially available compressed carbon monoxide often contains sufficient impurities, including sulfur compounds, to render its use in many catalytic reactions undesirable. Thompson (*82*) described an apparatus for preparing very pure carbon monoxide by decomposing formic acid in hot phosphoric acid. This method is laborious and requires relatively complicated apparatus for generating, storing, and compressing the carbon monoxide.

At this laboratory, mixtures of hydrogen and carbon monoxide of high purity (*26*) were prepared by reforming natural gas and then compressing it into conventional gas cylinders for use in catalyst studies. A simple system was developed for separating carbon monoxide from hydrogen at liquid-nitrogen temperatures and evaporating liquid carbon monoxide directly into a gas cylinder. As this method obviates the necessity for a gasholder and a compressor, the cost of the apparatus and installation was less than $500. About 100 cubic feet of pure carbon monoxide at 1,000 pounds per square inch gage can be prepared from $1H_2+3CO$ gas by one man in about 6 hours. The preparation requires 25 to 30 liters of liquid nitrogen.

A flow diagram of the apparatus is given in figure 35. A 2-liter condensation vessel was made from Schedule 80 stainless steel, type 304, by welding caps of the same material to a short section of tubing. This steel has high impact strength at low temperatures and is less likely to form carbonyls than carbon steels. A 1-liter purification vessel was fabricated from Schedule 80 carbon steel with provision for replacing absorbents. All components of the system were designed to withstand 3,000 pounds per square inch at room temperature.

The purification vessel was filled with about equal parts of activated carbon, Ascarite, and silica gel. The principal function of the adsorbents was to remove traces of water and carbon dioxide to prevent plugging of the inlet or outlet tubes of the condensation vessel; the secondary function was to remove traces of impurities such as sulfur compounds, if present.

Before the apparatus was used, the system was purged with synthesis gas by alternately increasing and lowering the pressure. The carbon monoxide cylinder either contained carbon monoxide or had been evacuated. The three-way needle valve, *A–D*, was closed. Needle valve *B* was opened to the synthesis gas cylinder, while pressure was being built up in the system. Valve *B* was closed, and liquid nitrogen was slowly poured into the Dewar flask. When the flask was filled, valve *B* was carefully opened to introduce additional synthesis gas slowly, so that the liquid nitrogen did not boil too rapidly. When the hydrogen pressure decreased the rate of condensation of carbon monoxide, residual hydrogen was slowly purged through valve *A*. The volume of gas thus removed was determined by a wet-test meter that indicated when the condensation vessel was filled with liquid carbon monoxide. Then valve *C* was closed, and the pressure in the condensation bomb was decreased to atmospheric pressure by opening valve *A*.

The liquid nitrogen bath was lowered from the condensation vessel, and enough liquid carbon monoxide was evaporated to purge residual hydrogen from the condensation vessel through valve *A*. *A* was closed, and the pressure in the condensation vessel was allowed to increase above the pressure in the cylinder containing carbon monoxide. Valve *D* and the valve at the cylinder containing carbon monoxide were opened, and carbon monoxide was evaporated into storage cylinders. When the pressure in this part of the system became constant, *D* was closed, and the condensation and evaporation procedures were repeated until the desired pressure was attained in the cylinder containing carbon monoxide.

Mass-spectrometric analysis of product gas showed 99.8 percent carbon monoxide, 0.15 percent hydrogen, and 0.05 percent methane. The efficiency of the process is about 80 percent, based on synthesis gas, and 18 percent, based on liquid nitrogen.

In the evaporation cycle, failure to open valve *D* or a plug in the tubing from the condensation vessel would result in excessive pressures in the condensation vessel. For this reason, the apparatus was installed in an area assigned to high-pressure experimentation, and during the evaporation cycle the operation was regulated from behind a protective barricade.

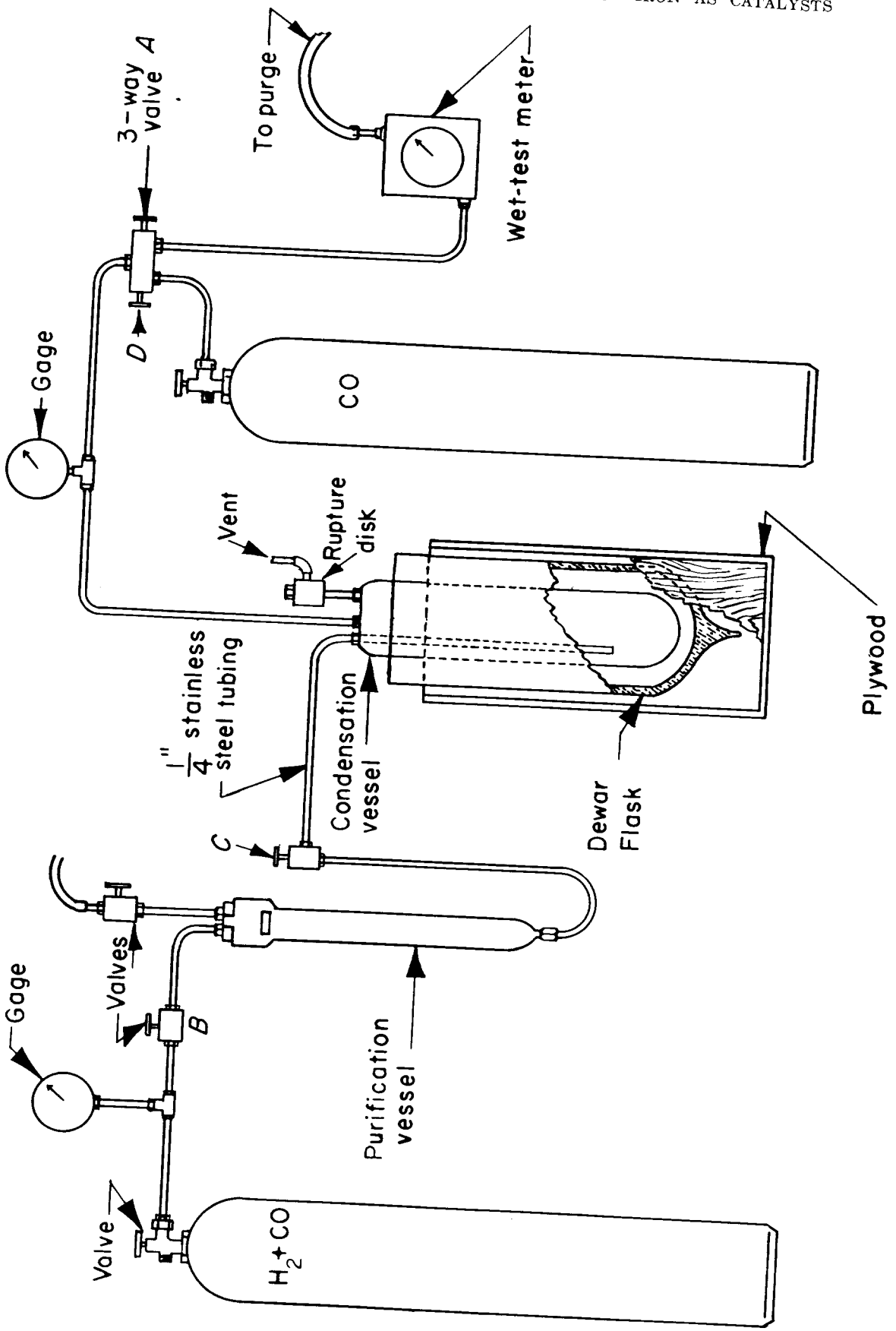

FIGURE 35.—Flow Diagram of Carbon Monoxide Separation From Synthesis Gas.

APPENDIX D.—CONSTANT LIQUID FEED SYSTEM

Frequently it is necessary to introduce small amounts of liquids into reaction systems at uniform rates. The simple glass apparatus (*77*) shown in figure 36 has been useful in catalytic studies at atmospheric pressure. Essentially the apparatus is in the form of a glass U-tube manometer with mercury acting as a piston to displace the liquid.

For the apparatus shown, a length of 2-mm. inside-diameter tubing is connected through stopcock *A* to a length of 20-mm. inside-diameter tubing. The liquid, to be fed into the system, is drawn into the 2-mm. tube by opening stopcock *B* to the liquid reservoir; *C*, to the tubing; and *A*, to the atmosphere. Finally, the level in the 2-mm. tubing is adjusted to zero. Stopcock *C* is then turned into the system. By adjusting stopcock *D* the flow of mercury can be regulated accurately enough to insure a constant liquid delivery rate. A further refinement in flow regulation can be obtained by placing a mercury filled leveling bottle above the mercury feed reservoir. A constant level can be maintained in the feed bottle by regulating the flow from the storage bulb.

It is evident that any flow rate desired can be obtained by using various conbinations of diameters of tubing. In the apparatus described, the areas of the tubing are in a ratio of 100 to 1. This arrangement permits delicate control of the feed rate.

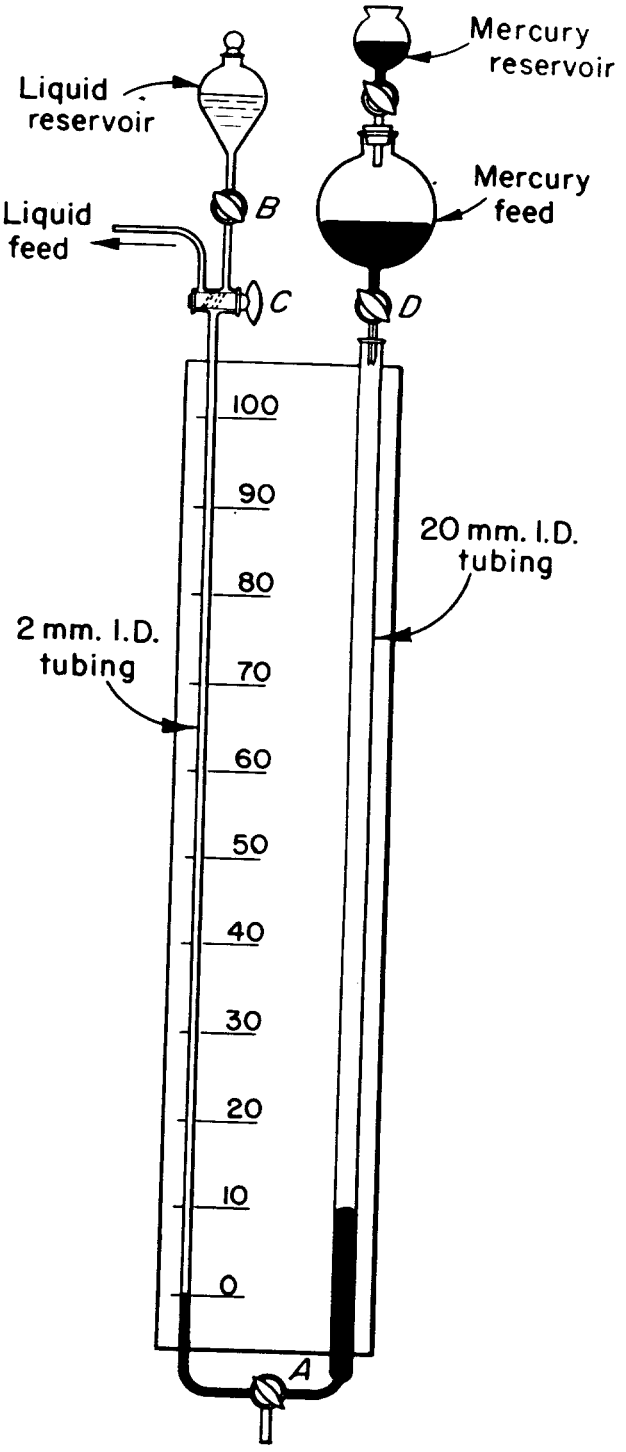

FIGURE 36.—Constant Liquid Feed System.

U.S. GOVERNMENT PRINTING OFFICE: 1963 O—683-935